Differential proteomics reveals age-dependent liver oxidative costs of innate immune activation in mice

Marine I. Plumel, Margaux Benhaim-Delarbre, Magali Rompais, Danièle Thiersé, Gabriele Sorci, Alain van Dorsselaer, François Criscuolo, Fabrice Bertile

Differential proteomics reveals age-dependent liver oxidative costs of immune activation in mice

Marine I Plumel[1,3], Margaux Benhaim-Delarbre[1,3], Magali Rompais[1,3], Danièle Thiersé[1,3], Gabriele Sorci[4], Alain van Dorsselaer[1,3], François Criscuolo[2,3$] and Fabrice Bertile[1,3*$]

[1] Institut Pluridisciplinaire Hubert Curien, Département Sciences Analytiques, CNRS UMR7178, 25 rue Becquerel, 67087 Strasbourg Cedex 2, France

[2] Institut Pluridisciplinaire Hubert Curien, Département d'Ecologie, Physiologie et Ethologie, CNRS UMR7178, 23 rue Becquerel, 67087 Strasbourg Cedex 2, France

[3] Université de Strasbourg, 4 rue Blaise Pascal, F-67081 Strasbourg Cedex, France

[4] Biogéosciences, CNRS UMR6282, Université de Bourgogne, 6 boulevard Gabriel, F-21000 Dijon, France

[$]: Equal contributors, shared seniorship of the paper

[*]: Corresponding author

Short title: Liver proteome changes during immune senescence

Keywords

Immunosenescence, liver, proteomics, oxidative stress, ageing, mice

Abstract

Individual response to an immune challenge results from the optimization of a trade-off between benefits and costs of immune cell activation. Immune-senescence can be viewed as the progressive loss of the fine-tuning of the immune system with age. Age-related immune complications may have several mechanistic bases, from immune cell defects to chronic pro-inflammatory status and oxidative imbalance, but we are still lacking experimental data showing the relative importance of each mechanism. Using a proteomic approach and subsequent biochemical validations of proteomics-derived hypotheses, we followed how 3-months and 1-year old-mice differed in their response to an acute innate immune challenge. Mice livers were collected 24 hours after immune priming and proteomic profiles were determined using 2D differential in-gel electrophoresis. Intensity of fifteen protein spots was shown to vary with age and immune treatment. Subsequent principal component analyses revealed that old mice present a chronic up-regulation of several proteins implicated in pathways related to oxidative stress control. Interestingly, these pathways were weakly affected by the immune challenge in old compared to young individuals. In addition, old mice suffered from lower glutathione-S-transferase activity and from higher oxidative damage at the end of the experiment, thus suggesting that they paid a higher immune-related cost than young individuals. On the whole, our data showed that a significant part of the liver costs elicited by an activation of the immune system is effectively related to oxidative stress, and that ageing impairs the capacity of old individuals to control it.

Significance

Our paper tackled the open question of the cost of mounting an innate immune response. Evolutionary biologists are familiar since a long time with the concept of trade-offs among key traits of an organism, trade-offs that shaped life history trajectories of species and individuals, ultimately in terms of reproduction and survival. On the other hands, medicine and molecular biologists studied the intimate mechanisms of immune senescence and underlined that oxidative imbalance is probably playing a key role in the progressive loss of immune function with age. This paper merges the two fields by exploring the nature of the cellular pathways that are mainly affected by age when the immune system is triggered. To do so, a proteomic approach was used to explore liver protein profiles and provide for the first time convincing data supporting the idea that oxidative stress constitutes a higher cost of immune response in old mice, possibly contributing to senescence. Proteomics-derived hypotheses were furthermore validated using biochemical assays. This paper therefore illustrates the adding value of using proteomics to answer evolutionary biology questions, and opens a promising way to study the inter-specific variability in the rates of immune-senescence produced by evolution.

Introduction

Senescence is a multi-level phenomenon that has cell roots and whole-organism ultimate impacts. It has been defined as the accumulation of unrepaired damages on biomolecules and cells causing the progressive decline of both organism functions and reproductive and survival rates of individuals over time [1]. Among the physiological functions shown to be affected by age, senescence of the immune system has been largely studied [2-4], and old individuals are often characterized by chronic or repeated infections, inflammatory diseases or autoimmune disorders [5]. In addition, the fact that senescent fibroblasts actually express inflammatory genes [6], suggest that even non-immune cells may contribute to mal-adaptive immunity in old-age individuals.

Interestingly, several studies from the molecular biology and medicine fields recently underlined that tackling the question of immune-senescence from an evolutionary point of view may help to better understand which mechanisms are important in the progressive impairment of the system [7; 8], and also whether the decrease in the immune reactiveness with age is mal-adaptive or not. More particularly, the well-known evolutionary concept of antagonistic pleiotropy [9] has been successfully applied to explain how some cell pathways may contribute to ageing. Those pathways have deleterious impact at old ages, but are still preserved by natural selection because of their beneficial effects on key life stages (in early life or during reproduction; e.g. TOR pathways, [10] and ultimately on overall individual fitness. Pleiotropy may also well explain why the control of the immune system is compromised with age, as strong responses are favoured by selection because of their efficiency in fighting parasites and diseases, but pro-inflammatory processes being also harmful in terms of co-lateral and auto-immune damage accumulation [11].

This idea of progressive accumulation of damage while growing old has also being theorized in the context of evolutionary biology, leading to the *Disposable Soma* theory [12]. While taking over the global idea of the *Antagonistic Pleiotropy* theory, Kirkwood gave a mechanistic explanation related to metabolism and direct negative impact of one function on another through the production of reactive oxygen species (ROS). ROS are inevitably produced by mitochondria when processing

reduced co-enzymes to ATP. Because functions compete for limited resources, this may reduce the investment an organism is currently doing in somatic maintenance, for example in buffering oxidants. This is even more critical when the activated physiological functions entail an increase in energy expenditure or produce the self-production of reactive species, both putatively modulating oxidative balance and ultimately ageing [13]. Such more or less clear relationships have been highlighted in laboratory and non-laboratory animal models [14-20], leading to the idea that oxidative stress could be one of the mediating mechanisms sustaining life-history trade-offs such as those among reproduction, growth or somatic maintenance and longevity [21].

Within somatic maintenance, the immune system has a preponderant role. It preserves the organism both from external (pathogens) and internal (cancer) threatens. Because immune response potentially implies the production of ROS both *via* an increased energy expenditure [22; 23] or the activation of immune cells [24; 25], mounting an immune response is likely to be costly and to lead to energy and oxidative based trade-offs. For instance, innate immunity relies on production of nitric oxide and superoxide by macrophages [26; 27] which may have non-specific deleterious impact on host cells [28]. However, individuals are not paying an identical energy cost when responding to an immune challenge, suggesting that old individuals may have to face more critical immune-associated trade-offs [23]. Such an observation suggests an ultimate cost of mounting an immune response, an idea further characterized in several taxa where individuals challenged with an immune treatment exhibit a reduced survival rate [29; 30], thereby underlying the key role of immune trade-off in shaping evolution patterns.

Senescence patterns are largely variable among species [31] but also within species among individuals [32], and the underlying mechanistic bases for such variability remain to date largely undefined, even if oxidative stress is likely to be of key importance [33]. As already done in previous studies of immune response mechanisms [34], we challenged here the immune system of mice using injections of lipopolysaccharide (LPS), a non-pathogen antigen, which is well known to trigger an innate inflammatory response. Previous studies in that field mostly considered measures at the

circulating level, showing for instance increased pro-oxidant impact [35], but also successfully characterizing proteomic specific patterns [36]. Based on this knowledge, one objective was therefore to decipher here liver regulations that are elicited in response to an immune challenge in mice. Indeed, the liver is a key organ for metabolic homeostasis maintenance, but it also has to constantly deal with antigenic loads [37; 38], and oxidative stress plays an important role in the pathogenesis of many liver diseases [39]. More particularly, the aim was to establish whether age-related changes in protein profiles could support the idea that old individuals actually pay a higher cost in terms of deleterious reactions triggered upon activation of the immune system (*e.g*. like oxidative imbalance) than young individuals. To do so, we took advantage of the benefits a global analytical strategy like proteomics can bring in the evolutionary ecology field [40].

Materials and Methods

Experimental procedures

The experiment was conducted using eight 3 month-old (young) and eight one year-old (old) C57BL/6J male mice, reared in our laboratory under constant temperature (24 ± 2 °C) and photoperiod (13:11 L:D cycle), with free access to food (SAFE A03) and water. Each group was randomly divided in two subgroups (4 mice each in separated cages) where animals received a single intraperitoneal injection of 25 µg/kg body mass LPS (from *E. Coli*, serotype 055-B5, patch 011M400IV, Sigma Aldrich), or phosphate buffered solution (PBS). This dose is largely below the lethal dose for young and 1 year-old mice (see [41]). None of the injected mice died after the injection. Body mass (± 0.1 g) of individuals was measured just before the injection and animal death. Mice were sacrificed 24h after injection by cervical dislocation and their liver was quickly collected, snap-frozen in liquid nitrogen, and several sample aliquots were stored at -80°C until biochemical and proteomic analyses. The study complied with legislation (L87-848) on animal experimentation in France and was done under the DEPE license obtained from the French Department of Veterinary Service (number G67-482-18). Dr François Criscuolo is the holder of an animal experimentation license (n°67-78) delivered by French authorities.

Liver proteomics

Unless otherwise specified, all chemicals and reagents were purchased from Sigma Aldrich (St. Louis, MO, USA).

Protein extraction. Frozen liver samples were first pulverized using a laboratory ball mill (Mikrodismembrator, Sartorius). ~10mg of the grinded powders were then dissolved in 400 µL of a buffer composed of 8M Urea, 2M Thiourea, 4% Chaps, 1% dithiothreitol, Triton X100 0.5%, TLCK 0.05% and 0.02 to 2 mM protease inhibitors. After sonication on ice (10 s, 135 watts), 9 volumes of cold acetone were added, and samples were kept at -20°C during 16h. Proteins were pelleted by centrifugation (14 min, 4°C, 14000 g), vacuum-dried (Speedvac, Thermoscientific) after discarding

supernatants, and then dissolved in a buffer composed of 7M Urea, 2M Thiourea, 30mM Tris (pH 8.5) and 4% Chaps buffer. After adjustment of the pH to 8.5, homogenization was finally completed by sonication on ice (10 s, 135 watts).

After determination of total protein concentrations using the Bio-Rad Protein Assay (BioRad, Hercules, CA, USA), protein integrity and similarity of electrophoretic protein profiles was checked prior to 2D-DIGE analysis. To do so, proteins were electrophoresed on a 12% SDS-PAGE acrylamide gel (20 µg loaded; 50 V for 30 min and then 100 V to complete migration) and stained with Coomassie blue.

2D-DIGE experiment. Protein samples were first labelled using a CyDye DIGE Fluor Minimal Dye Labeling Kit (GE HealthCare, Uppsala, Sweden). More precisely, 400 pmol of Cy3 and Cy5 were used to randomly label 50 µg of protein samples from the different groups, and 3.2 nmol of Cy2 were used to label 400 µg of proteins after having mixed all the samples (25µg each; internal standard). After incubation in the dark for 30 min on ice, protein labelling was quenched by addition of 10 mM lysine and incubation in the dark for 10 min on ice. Random distribution of samples from the 4 groups (i.e. young PBS, yound LPS, old PBS and old LPS) was by mixing and diluting 50 µg of Cy2, Cy3 and Cy5-labelled protein samples in 400 µL of a buffer composed of 7M urea, 2M thiourea, 2% Chaps, 2% DTT, 2% ampholytes (Amersham Pharmacia-Biotech, Uppsala, Sweden), and a trace of bromophenol blue. Loading onto 18cm pH3-10 non-linear immobilized pH gradient strips (IPG Ready strip, Biorad, Hercules, CA, USA), was then followed by passive rehydration over 2h30 in the dark prior to active rehydration overnight by applying a voltage of 50V using a Protean IEF cell (Biorad, Hercules, CA, USA). Isoelectric focusing (IEF) was afterwards performed until reaching a total focusing time of 85000 Vh, by applying voltage gradient steps (from 0 to 200V in 1h, from 200 to 1000 V in 4h, from 1000 to 5000 V in 16h, then 5000V for 7h). Focused proteins were then reduced and alkylated through a first incubation of IPG strips in a buffer composed of 1% DTT, 6M Urea, 50mM Tris pH 8.8, 30% glycerol and 2% SDS during 30 min, and a second incubation in a buffer composed of 2,5 %

iodoacetamide, 6M Urea, 50mM Tris pH 8.8, 30% glycerol and 2% SDS during 30 min. IPG strips were then sealed onto 10% polyacrylamide SDS-PAGE gels (20 x 20 cm) with 0.5% agarose, and focused proteins were electrophoresed using a Protean II xi Cell (Biorad Hercules, CA, USA) by application of 5 mA per gel for 1h followed by 8mA per gel for 8h.

Another 2D-gel was run in parallel, on which a larger amount of proteins (i.e. 1 mg of the non-labelled internal standard) was loaded. It was used to specifically improve quality of mass spectrometry-based protein identifications.

Quantitative analysis from 2D-gel images. After electrophoresis, gels were washed with water and gel images were acquired at 100 µm resolution (Ettan DIGE Imager, Ge Healthcare Uppsala, Sweden). Using Progenesis Samespots (v4.5, Nonlinear dynamics, Newcastle, UK), image quality was first controlled and all images were automatically aligned, with subsequent minor "hand-made" adjustments to improve accuracy of alignments. Background subtraction was then followed by normalization of Cy3 and Cy5 spot volumes to those of corresponding Cy2 spots, and application of a correction based on 1) the calculation of the global distribution of all Cy3/Cy2 and Cy5/Cy2 ratios and 2) the determination of a global scaling factor for all gels. Hence, any possible inter-gel variations were eliminated and accurate quantitative data were obtained.

nanoLC-MS/MS analyses. After automatic excision of differential protein spots (see Statistics) using an automated gel cutter (PROTEINEER sp, Bruker Daltonics, Bremen, Germany), a Massprep Station (Waters, MicroMass, Manchester, UK) was used first to apply 3 wash cycles (10 min each) in 50 µL of 25 mM NH_4HCO_3 and 50 µL of acetonitrile, followed by a dehydration step (50 µL acetonitrile, 60°C, 5 min). Destaining was then followed by in-gel reduction (incubation at 60°C for 30 min in 50 µL of 10mM DTT, 25mM NH_4HCO_3) and in-gel alkylation (incubation 30 min in 55mM iodoacetamide, 25 mM NH_4HCO_3) of proteins using the same Massprep Station. A last washing step (10 min) in 50 µL of 25 mM NH_4HCO_3 and 50 µL of acetonitrile, followed by gel spots dehydration during 15 min in 50 µL

of acetonitrile were then carried out before in-gel protein digestion (5h at 37°C) using trypsin (Promega, Madison, WI, USA) diluted in 25 mM NH_4HCO_3. The resulting tryptic peptides were then extracted using 30µL of a 60% acetonitrile solution containing 0.1% of formic acid. Acetonitrile was removed by vacuum drying using a speedvac.

A 1200 series nanoHPLC-Chip system (Agilent Technologies, Palo Alto, CA, USA) coupled to an HCT™ Plus ion trap (Bruker Daltonics, Bremen, Germany) was used to analyze tryptic peptides. The solvent system consisted of 2% acetonitrile, 0.1% HCOOH in water (solvent A) and 2% water, 0.1% formic acid in acetonitrile (solvent B). After loading of 3 µL of samples onto the enrichment column (ZORBAX 300SB-C18, 40 nL, 4 mm, with a 5 µm particle size) at a flow rate of 3.75 µL / min with solvent B, elution was performed on a separation column (ZORBAX 300SB-C18, 43 mm x 75 µm, with a 5 µm particle size) at a flow rate of 300 nL/min, according to the following gradient steps: From 8% to 40% B in 7 min, then from 40% to 70% B in one min, then 70% B during 2 min.

The mass spectrometer was operated with automatic switching between MS and MS/MS modes. The following voltages were set up: -1800 V (inlet), +147.3 V (outlet) and a skimmer voltage of +40V. For mass spectrometry data acquisition, the scan speed was set at 8100 m/z per sec in the MS mode and 26000 m/z per sec in the MS/MS mode. Mass range was set at 250-2000 m/z in the MS mode and 50-2800 m/z in the MS/MS mode. The 3 most intense ions (doubly charged) were selected for CID-based fragmentation, and exclusion was set at 1 min or 2 spectra. The system was fully controlled by ChemStation (Rev B.01.035R1) and EsquireControl (v5.3) software (Agilent technologies and Bruker Daltonics, respectively).

MS/MS data analysis. Two different algorithms were used to analyze MS/MS data. The Mascot™ v2.3.02 program (Matrix Science, London, UK) was installed on a local server and the OMSSA v2.1.7 program (Open Mass Spectrometry Search Algorithm) [42] was run using the MSDA software suite [43]. Data were searched against a target-decoy version of the *Mus musculus* (Taxonomy 10090) protein database downloaded from NCBInr containing common contaminants like keratins and

trypsin (July 2015, 410544 target+decoy entries), with a mass tolerance of 0.25 Da in MS and MS/MS modes, and allowing a maximum of one trypsin missed cleavage. Optional modifications were set as follows: carbamidomethylation of cysteine residues, oxidation of methionine residues, and acetylation of protein N-termini. Stringent filtering criteria based on probability-based scoring of the identified peptides were applied using Scaffold software v.3.0.7 (Proteome software Inc., Portland, OR, USA), to obtain a FDR < 1%. Hence, single peptide-based identifications were validated for MS/MS ion scores higher than 45 (Mascot) and –logE values higher than 5.3 (Omssa). Multiple peptide-based identifications were validated for MS/MS ion scores higher than 30 (Mascot) and –logE values higher than -0.05 (Omssa). Common contaminants such as keratin and trypsin were not considered.

When several different proteins were identified from analysis of a same protein spot, the so-called major ones (supposedly more abundant and responsible of possible spot intensity variation) were determined through a "peptide counting strategy" considering the percentage of experimentally detected peptides per protein (Mascot + Omssa) relative to the theoretical detectable number. To compute the theoretical number of detectable tryptic peptides, the possible presence of a Proline after a tryptic sites was considered, one missed cleavages was allowed, and the adequate size of peptides for their detection by mass spectrometry was determined directly from our data, which identified peptides composed of 5-33 amino acids. Hence, we calculated similar theoretical numbers of detectable tryptic peptides between major (69 ± 2) and minor (73 ± 3) proteins. Here, the proteins that were considered as major ones in a given protein spot were those to which about three times more peptides had been assigned versus minor ones (22 ± 1 % vs. only 8 ± 1 % of the possible tryptic peptides, respectively).

Body mass and biochemical validation of proteomic-derived hypothesis

Body mass loss (expressed in g) was recorded over the 24 hour treatment to evaluate energy cost of the immune response to the LPS injection. Biochemical measurements in liver samples were done in

duplicate using assay kits purchased from Cayman Chemical (Ann Arbor, MI, USA). First, to confirm that variations in protein abundances were consistent with corresponding variations in protein activity, total glutathione S-transferase activity was assessed. To further validate the hypothesis on oxidative stress, reduced (GSH) and oxidized (GSSG) glutathione contents were measured in mice liver and liver protein carbonyl content was also measured as it is a commonly used marker of ROS-induced protein oxidation.

Statistical analysis

Body mass loss, biochemical and proteomic data were first checked for differences among groups using ANOVA with Age (young and old) and treatment (LPS and PBS) as fixed factors. In a second step, we then decided to run two Principal Component Analyses (PCA) with varimax rotation separately with a PCA conducted on the body mass loss and biochemical data (PCA1) and a PCA with only the restricted number of differential (i.e. significant) protein spots (PCA2). PCA resulted in two (PCA1) and three (PCA2) orthogonal variables (components, PCs) allowing easier comparisons of overall differences in liver biochemical and proteomic profiles among groups. Determinants of PCA1 and PCA2 were greater than 0.00001 (1.00×10^{-3} and 1.89×10^{-3}, respectively), Kaiser-Meyer-Olkin measures showed sample adequacy for the analysis (0.71 and 0.61, respectively), individual items KMO values were > 0.66 (PCA1) and > 0.53 (PCA2) and Bartlett's test of sphericity showed sufficiently large correlation among variables for PCA (χ^2 (10) = 97.898, $P < 0.001$, χ^2 (66) = 135.684, $P < 0.001$, respectively). Only components with eigenvalues which met the Kaiser's criterion of 1 were conserved to explain total variance of the data. Subsequently, PCA scores of each individual were analysed by using Generalized Linear Model with Age, treatment and Age x Treatment interaction to check for differences in response to LPS. When the interaction was found significant, posthoc comparisons were conducted using the same model but separated by Age or Treatment. Normality was tested for all models on residuals, using Kolmogorov-Smirnov test and checking linearity of QQ plots. Significance threshold is $P < 0.054$.

Results

Immune challenge-induced liver proteome changes

Multiple ANOVA analysis applied to relative intensities of 384 detected 2D-DIGE protein spots revealed that 17 of them exhibited significant differences among old and young mice treated with PBS or LPS ($P < 0.05$; **Table 1**). These 17 protein spots (**Figure 1**) contained 18 different proteins, which were unambiguously identified on the basis of mass spectrometry data analysis (see **Supplementary Table 1** for details). Most of these 18 liver proteins are known to play key roles in the response to oxidative stress, in energy metabolism and in the response to immune challenges, which suggest involvement of these biological processes when immune system is activated.

To further understand phenotypic responses in immune-challenged (LPS) old and young mice, PCA analysis was run using only 15 of the 17 differential protein spots. Indeed, protein spots N°459 and N°510 were not considered here because they rendered the definite matrix non-positive. Three components (PC1, PC2, and PC3) with eigenvalues higher than 1, and explaining 79% of the total variance after rotation, were obtained (**Table 2**). Only protein loadings over 0.6 were considered due to relatively small sample size [44], which allowed changes in liver protein abundances to be attributed to either of the 3 principal components. Particular biological processes were then linked to each of the principal components, on the basis of GO ontologies (extracted using the MSDA software suite [43]) and literature examination. Hence, our results suggest that PC1 is especially related to response to oxidative stress, PC2 to both response to oxidative stress and energy metabolism, and PC3 to both response to oxidative stress and immune challenge.

To better determine how the 3 components were altered by LPS immune challenge in old and young mice, generalized linear models were run (**Table 3**). A significant effect of Treatment (LPS or PBS) on PC1 and PC2 was found, while Age had a significant effect only on PC3. Interaction Age x Treatment was significant for PC1 and PC3. Thus, young and old mice responded differently to LPS injections with regard to PC1 (PC1 indices significantly decreased in young LPS mice while did not change in old mice; **Figure 2**). More precisely, levels of 3-hydroxyanthranilate 3,4-dioxygenase, Glutathione-S-

transferase, Peroxiredoxin-6 and Carbonic anhydrase 3 being significantly reduced while those of 78 kDa glucose-regulated protein (GRP-78) were increased only in LPS-injected young mice vs. PBS-injected young mice (**Table 2 and Figure 2**). PC2 indices were higher in both old and young LPS-injected animals (**Figure 2**), thus suggesting that LPS injections had a comparable effect whatever the age of mice, levels of Glutathione synthetase, S-adenosylmethionine synthase isoform type-1, and Fibrinogen alpha polypeptide isoform 2 precursor + Propanoyl-CoA C-acyltransferase + NADP-dependent malic enzyme being increased while those of Sorbitol dehydrogenase precursor are decreased in LPS-injected vs. PBS-injected mice (**Table 2 and Figure 2**). Finally, PC3 indices were globally higher in older mice (**Figure 2**), suggesting that levels of mitochondrial aldehyde dehydrogenase and Dihydrolipoyl dehydrogenase + Prolyl aminopeptidase + Fibrinogen beta chain are higher while those of Glycine N-methyltransferase are lower in old vs. young mice (**Table 2**). In addition, the significant interaction Age x Treatment indicated that old individuals, despite preserving higher PC3 values, exhibited a decrease after injection while young individuals significantly increased their PC3 levels (**Table 3 and Figure 2**).

Thus, proteomics data analysis led to the hypothesis that oxidative balance is adjusted upon LPS treatment, but especially in young animals where response to endoplasmic reticulum (ER) stress would be higher. Proteomics data also indicate a stressed oxidative status in relation to immune challenge pre-exists in old mice before LPS injection. Altogether, these data strongly support that LPS treatment induces liver oxidative stress, but also that ageing is associated with different pre- and post-LPS injection oxidative status. To test this hypothesis, liver oxidative stress-related proxies were assessed.

Immune challenge-induced liver oxidative stress

For a given age, initial body masses were not different between LPS- and PBS-mice (GLM, $F_{1, 15} = 1.08$, $P = 0.319$). Old individuals were shown to have a higher body mass than young individuals, irrespectively of the immune treatment (GLM, $F_{1, 15} = 5.00$, $P < 0.001$; estimates 10.19 ± 2.04). PCA2

analysis using body mass loss and liver oxidative stress-related measurements produced two components (PC1 and PC2) with eigenvalues higher than 1, and explaining 87% of the total variance (**Table 2**). Considering only factor loadings over 0.6 (see above), we found that PC1 was related to body mass loss and levels of total GSH, GSSG and protein carbonyl. PC2 was here related to Glutathione-S-transferase activity.

Generalized linear models revealed a significant effect of Treatment (LPS or PBS) on PC1, while Age had a significant effect only on PC2 (**Table 4**). Interaction Age x Treatment was significant only for PC1. Thus, young and old mice responded differently to LPS injections with regard to PC1, PC1 indices being lower in LPS *vs.* PBS mice, but with a more marked drop in old LPS-treated animals (**Figure 3**). It means that body mass loss was more pronounced and levels of total GSH and GSSG were significantly more decreased in LPS-injected vs. PBS-injected old mice than in LPS-injected vs. PBS-injected young mice (**Table 2 and Figure 3**). In the same time, oxidative damages on liver proteins (protein carbonyl contents) were more markedly increased in older mice after LPS injection. PC2 indices were higher only in young PBS-injected mice (**Figure 3**), suggesting that old mice have lower Glutathione-S-transferase activity than younger individuals (**Table 2 and Figure 3**).

Thus, our biochemical tests confirmed proteomics-driven hypothesis that LPS treatment induces liver oxidative stress, and that this effect is more marked in older mice due to a lack of antioxidant capacities.

Discussion

The present study strongly suggests that activation of the immune system in mice triggers several cellular and metabolic pathways that are all related to a response to oxidative stress. In addition, one other important conclusion is that 1 year-old individuals do not exhibit marked changes in their liver protein profiles 24-h after LPS injection, suggesting that they have lost part of their immune responsiveness. This is corroborated by the fact that old individuals had higher body mass loss after injection than young ones, which would indicate a slower cleaning-up of LPS by their immune system. Consequently, LPS-challenged old-individuals pay a higher immune cost in terms of oxidative stress, as reflected by higher protein carbonyl levels and lower GST activity in liver homogenates. We also detected higher levels of proteins related to oxidative stress control in old individuals independently of immune treatment, suggesting constitutive costs associated to dysregulation of immune-related parameters even in the absence of pathogen. Our study therefore brings to the fore proteomic proofs that preserving immune efficiency at old age in mice may trigger oxidative imbalance.

Demonstrating that immune defence is costly in animals is still under debate [45; 46], despite some evidence for anti-parasite activities [47; 48]. The idea developed here is that immune activation is competing for limited energy resources, thereby entailing a cost for the host. Our proteomic data pointed out that abundance of several proteins was changed independently of age following LPS injection, with proteins related to oxidative stress and energy metabolism (PCA1, PC2), rather suggesting that carbohydrate (and possibly fatty acid) metabolism is enhanced (Tables 1 and 2). It is interesting to note that fibrinogen alpha-2 precursor could also be positively affected by LPS injection, underlying that the preservation of hemostasis could be an important feature of the immune response. However, an experiment conducted on Blue Tit (*Parus caeruleus*) found rather weak energy cost of immune (antibody) response (<13% of the basal metabolic rate) and suggested that non-energetically driven trade-offs may be more constraining for the immune system [49]. Among different possibilities (see [50] for an alternative explanation), the by-production of ROS either because of the increase in metabolic rate or directly by immune cells has been previously

proposed to be particularly deleterious [51]. For example, immune system regulation largely depends on the ability of a large number of cell types to produce nitric oxide (such as fibroblasts, macrophages, natural killer cells) either to regulate cell activation/proliferation (*e.g.* T lymphocytes) or to destroy infectious organisms [52]. The absence of tightly coordinated or well-balanced control of immune-induced ROS production may lead to damage accumulation, thereby accounting for immune trade-offs [53; 54]. Interestingly, this deleterious phenomenon may particularly take place when individuals are in bad conditions, either because of environmental energy constraints or of a decrease in organism functionality with age. Indeed, autoimmune (oxidative-derived) damage remains one of the main consequences of immune-senescence in old-individuals [51]. In both young and old mice, proteomics data suggest that LPS treatment would trigger synthesis of glutathione, an important antioxidant [55], and of S-Adenosylmethionine, which can potentiate activity of antioxidant enzymes [56; 57]. Therefore, enhancing antioxidant capacities seems to be an important regulating feature when mounting an innate immune response. However, young and old mice did not respond identically. Old mice showed very little changes in their protein profiles related to response to oxidative stress. For instance, proteins like mitochondrial aldehyde dehydrogenase, peroredoxin-6 or glutathione-S-transferase were all mobilized in young individuals whereas they were not changed significantly in old LPS-treated animals. These proteins are either antioxidant enzymes or involved in mitochondrial protection against oxidative stress [58], suggesting that old mice have lost part of the antioxidant barrier that must come with immune response. Oxidative cost of badly tuned immune response could damage irreversibly some key ageing markers, with particular deleterious impact for immune cells themselves. Shortened telomere ends of linear chromosomes may reduce T- and B-lymphocytes proliferative capacity, thereby contributing to defective immune response in old-individuals [59]. We reach here one limitation of our study since we did not detect any specific immune markers to vary among groups, or target immune tissue for proteomic analysis. Therefore, weather macrophage, natural killers or lymphocytes populations in old mice have decreased cell proliferation because of enhanced senescence rate remains an open question for which proteomic

has clearly a role to play. There are anyway two interesting points to note coming from our data. First, that old animals, in addition to their weak protein response to LPS, also have basal higher protein carbonyl values than young individuals, indicating that oxidative stress related-pathways are chronically enhanced. Such age-related cost could partly be attributable to a putative high constitutive immune cost in aging animals, i.e. related to the maintenance of the immune system in the absence of pathogen [60]. Secondly, we found a chaperon protein, GRP-78 likely to be more expressed in young animals after LPS injection. This protein is associated at the cell surface with major histocompatibility class 1 molecule, suggesting a role in cell immune response [61]. In addition, GRP-78 may also fulfil a protective role against endoplasmic reticulum stress-induced cell death [62]. This indicates an interesting mechanism linking immunity and body maintenance that should be more precisely studied in the context of trade-offs between immunity and other life history traits.

Conclusions

In the present study, we used a proteomic approach to further characterize in mice liver the protein pathways that may be differently affected by the trade-off between body maintenance and an innate immune response in relation with age. We highlighted that most of the differential protein spots contain proteins that are related to the control of the oxidative status of the individual. In old animals prior to the injection, those pathways appeared enhanced, and then were only weakly modified by the LPS challenge. This is likely to be associated to a higher oxidative stress paid as a cost of constitutive immune maintenance, as shown by our biochemical measurements. Interestingly, we also highlighted one new way through which immunity and lifespan may be trade-offed, *via* the regulation of the GRP-78 chaperon protein, illustrating the plus-value of applying proteomics to evolutionary biology questions. A coming step will be to both explore immune trade-offs in other organisms with contrasting lifespans (i.e. birds) using the same methodology, to better determine the nature of the mechanisms on which are based immune costs [47; 60; 63-65], and how they have been modified by species evolutionary history.

Supplementary data

Supplementary Table 1. List of identified proteins and their annotations from differential 2D-DIGE protein spots

Competing interest statement

The authors declare that they have no competing interests

Acknowledgements

This work was supported by the CNRS and Strasbourg University (H2E project; IDEX UNISTRA), the French Proteomic Infrastructure (ProFI; ANR-10-INSB-08-03), and a CNRS "Projets Exploratoires Premier Soutien" (PEPS). We wish to thank Aurélie Hranitsky for her contribution with animal husbandry.

References

[1] Finkel T, Holbrook NJ Oxidants, oxidative stress and the biology of ageing. Nature 2000;*408*(6809):239-247.

[2] Blasco MA Immunosenescence phenotypes in the telomerase knockout mouse. Springer Semin Immunopathol 2002;*24*(1):75-85.

[3] Lasry A, Ben-Neriah Y Senescence-associated inflammatory responses: aging and cancer perspectives. Trends Immunol 2015;*36*(4):217-228.

[4] Miller RA The aging immune system: primer and prospectus. Science 1996;*273*(5271):70-74.

[5] Caruso C, Buffa S, Candore G, Colonna-Romano G, Dunn-Walters D, Kipling D, Pawelec G Mechanisms of immunosenescence. Immun Ageing 2009;*6*:10.

[6] Shelton DN, Chang E, Whittier PS, Choi D, Funk WD Microarray analysis of replicative senescence. Curr Biol 1999;*9*(17):939-945.

[7] Weng NP Aging of the immune system: how much can the adaptive immune system adapt? Immunity 2006;*24*(5):495-499.

[8] Shanley DP, Aw D, Manley NR, Palmer DB An evolutionary perspective on the mechanisms of immunosenescence. Trends Immunol 2009;*30*(7):374-381.

[9] Williams GC Pleiotropy, natural selection, and the evolution of senescence. Evolution 1957;*11*:398-411.

[10] Blagosklonny MV Revisiting the antagonistic pleiotropy theory of aging TOR-driven program and quasi-program. Cell Cycle 2010;*9*(16):3151-3156.

[11] Licastro F, Candore G, Lio D, Porcellini E, Colonna-Romano G, Franceschi C, Caruso C Innate immunity and inflammation in ageing: a key for understanding age-related diseases. Immun Ageing 2005;*2*:8.

[12] Kirkwood TB Evolution of ageing. Nature 1977;*270*(5635):301-304.

[13] Harman D Aging: a theory based on free radical and radiation chemistry. J Gerontol 1956;*11*(3):298-300.

[14] Alonso-Alvarez C, Bertrand S, devevey G, Prost J, Faivre B, Sorci G Increased susceptibility to oxidative stress as a proximate cost of reproduction. Ecology Letters 2004;*7*:363-368.

[15] Alonso-Alvarez C, Bertrand S, Faivre B, Sorci G Increased susceptibility to oxidative damage as a cost of accelerated somatic growth in zebra finches. Funct Ecol 2007;*21*(5):873-879.

[16] Costantini D, Dell'Omo G Effects of T-cell-mediated immune response on avian oxidative stress. Comp Biochem Physiol A Mol Integr Physiol 2006;*145*(1):137-142.

[17] Hamilton ML, Van Remmen H, Drake JA, Yang H, Guo ZM, Kewitt K, Walter CA, Richardson A Does oxidative damage to DNA increase with age? Proc Natl Acad Sci U S A 2001;*98*(18):10469-10474.

[18] Klandorf H, Rathore DS, Iqbal M, Shi X, Van Dyke K Accelerated tissue aging and increased oxidative stress in broiler chickens fed allopurinol. Comp Biochem Physiol C Toxicol Pharmacol 2001;*129*(2):93-104.

[19] Le Bourg E Oxidative stress, aging and longevity in Drosophila melanogaster. FEBS Lett 2001;*498*(2-3):183-186.

[20] Wiersma P, Selman C, Speakman JR, Verhulst S Birds sacrifice oxidative protection for reproduction. Proc Biol Sci 2004;*271 Suppl 5*:S360-363.

[21] Monaghan P, Metcalfe NB, Torres R Oxidative stress as a mediator of life history trade-offs: mechanisms, measurements and interpretation. Ecol Lett 2009;*12*(1):75-92.

[22] Martin LB, Scheuerlein A, Wikelski M Immune activity elevates energy expenditure of house sparrows: a link between direct and indirect costs? P Roy Soc B-Biol Sci 2003;*270*(1511):153-158.

[23] Demas GE, Chefer V, Talan MI, Nelson RJ Metabolic costs of mounting an antigen-stimulated immune response in adult and aged C57BL/6J mice. Am J Physiol 1997;*273*(5 Pt 2):R1631-1637.

[24] De la Fuente M Effects of antioxidants on immune system ageing. Eur J Clin Nutr 2002;*56 Suppl 3*:S5-8.

[25] Emre Y, Hurtaud C, Nubel T, Criscuolo F, Ricquier D, Cassard-Doulcier AM Mitochondria contribute to LPS-induced MAPK activation via uncoupling protein UCP2 in macrophages. Biochem J 2007;*402*(2):271-278.

[26] Gordon S Alternative activation of macrophages. Nat Rev Immunol 2003;*3*(1):23-35.

[27] Lambeth JD NOX enzymes and the biology of reactive oxygen. Nat Rev Immunol 2004;*4*(3):181-189.

[28] Lambeth JD, Krause KH, Clark RA NOX enzymes as novel targets for drug development. Semin Immunopathol 2008;*30*(3):339-363.

[29] Hanssen SA, Hasselquist D, Folstad I, Erikstad KE Costs of immunity: immune responsiveness reduces survival in a vertebrate. P Roy Soc B-Biol Sci 2004;*271*(1542):925-930.

[30] Moret Y, Schmid-Hempel P Survival for immunity: The price of immune system activation for bumblebee workers. Science 2000;*290*(5494):1166-1168.

[31] Vleck CM, Haussmann MF, Vleck D Avian senescence: underlying mechanisms. J Ornithol 2007;*148*:S611-S624.

[32] Bouwhuis S, Charmantier A, Verhulst S, Sheldon BC Individual variation in rates of senescence: natal origin effects and disposable soma in a wild bird population. J Anim Ecol 2010;*79*(6):1251-1261.

[33] Bize P, Cotting S, Devevey G, van Rooyen J, Lalubin F, Glaizot O, Christe P Senescence in cell oxidative status in two bird species with contrasting life expectancy. Oecologia 2014;*174*(4):1097-1105.

[34] Janeway CA, Jr., Medzhitov R Innate immune recognition. Annu Rev Immunol 2002;*20*:197-216.

[35] Bai Y, Onuma H, Bai X, Medvedev AV, Misukonis M, Weinberg JB, Cao W, Robidoux J, Floering LM, Daniel KW, Collins S Persistent nuclear factor-kappa B activation in Ucp2-/- mice leads to enhanced nitric oxide and inflammatory cytokine production. J Biol Chem 2005;*280*(19):19062-19069.

[36] Oveland E, Karlsen TV, Haslene-Hox H, Semaeva E, Janaczyk B, Tenstad O, Wiig H Proteomic evaluation of inflammatory proteins in rat spleen interstitial fluid and lymph during LPS-induced systemic inflammation reveals increased levels of ADAMST1. J Proteome Res 2012;*11*(11):5338-5349.

[37] Liaskou E, Wilson DV, Oo YH Innate immune cells in liver inflammation. Mediators Inflamm 2012;*2012*:949157.

[38] Racanelli V, Rehermann B The liver as an immunological organ. Hepatology 2006;*43*(2 Suppl 1):S54-62.

[39] Tanikawa K, Torimura T Studies on oxidative stress in liver diseases: important future trends in liver research. Med Mol Morphol 2006;*39*(1):22-27.

[40] Diz AP, Martinez-Fernandez M, Rolan-Alvarez E Proteomics in evolutionary ecology: linking the genotype with the phenotype. Mol Ecol 2012;*21*(5):1060-1080.

[41] Belloni V, Faivre B, Guerreiro R, Arnoux E, Bellenger J, Sorci G Suppressing an anti-inflammatory cytokine reveals a strong age-dependent survival cost in mice. PLoS One 2010;*5*(9):e12940.

[42] Geer LY, Markey SP, Kowalak JA, Wagner L, Xu M, Maynard DM, Yang X, Shi W, Bryant SH Open mass spectrometry search algorithm. J Proteome Res 2004;*3*(5):958-964.

[43] Carapito C, Burel A, Guterl P, Walter A, Varrier F, Bertile F, Van Dorsselaer A MSDA, a proteomics software suite for in-depth Mass Spectrometry Data Analysis using grid computing. Proteomics 2014;*14*(9):1014-1019.

[44] Field A Discovering Statistics Using SPSS. Second Edition. Sage Publications, Ltd 2009.

[45] Rigby MC, Hechinger RF, Stevens L Why should parasite resistance be costly? Trends Parasitol 2002;*18*(3):116-120.

[46] Williams TD, Christians JK, Aiken JJ, Evanson M Enhanced immune function does not depress reproductive output. P Roy Soc B-Biol Sci 1999;*266*(1420):753-757.

[47] Lochmiller RL, Deerenberg C Trade-offs in evolutionary immunology: just what is the cost of immunity? Oikos 2000;*88*(1):87-98.

[48] Sheldon BC, Verhulst S Ecological immunology: costly parasite defences and trade-offs in evolutionary ecology. Trends Ecol Evol 1996;*11*(8):317-321.

[49] Svensson E, Raberg L, Koch C, Hasselquist D Energetic stress, immunosuppression and the costs of an antibody response. Funct Ecol 1998;*12*(6):912-919.

[50] Adamo SA, Roberts JL, Easy RH, Ross NW Competition between immune function and lipid transport for the protein apolipophorin III leads to stress-induced immunosuppression in crickets. J Exp Biol 2008;*211*(Pt 4):531-538.

[51] Sadd BM, Siva-Jothy MT Self-harm caused by an insect's innate immunity. Proc Biol Sci 2006;*273*(1600):2571-2574.

[52] Coleman JW Nitric oxide in immunity and inflammation. Int Immunopharmacol 2001;*1*(8):1397-1406.

[53] von Schantz T, Bensch S, Grahn M, Hasselquist D, Wittzell H Good genes, oxidative stress and condition-dependent sexual signals. Proc Biol Sci 1999;*266*(1414):1-12.

[54] Dowling DK, Simmons LW Reactive oxygen species as universal constraints in life-history evolution. Proc Biol Sci 2009;*276*(1663):1737-1745.

[55] Mari M, Morales A, Colell A, Garcia-Ruiz C, Fernandez-Checa JC Mitochondrial glutathione, a key survival antioxidant. Antioxid Redox Signal 2009;*11*(11):2685-2700.

[56] Cavallaro RA, Fuso A, Nicolia V, Scarpa S S-adenosylmethionine prevents oxidative stress and modulates glutathione metabolism in TgCRND8 mice fed a B-vitamin deficient diet. J Alzheimers Dis 2010;*20*(4):997-1002.

[57] Caro AA, Cederbaum AI Antioxidant properties of S-adenosyl-L-methionine in Fe(2+)-initiated oxidations. Free Radic Biol Med 2004;*36*(10):1303-1316.

[58] Ohsawa I, Nishimaki K, Yasuda C, Kamino K, Ohta S Deficiency in a mitochondrial aldehyde dehydrogenase increases vulnerability to oxidative stress in PC12 cells. J Neurochem 2003;*84*(5):1110-1117.

[59] Goronzy JJ, Fujii H, Weyand CM Telomeres, immune aging and autoimmunity. Exp Gerontol 2006;*41*(3):246-251.

[60] Sandland GJ, Minchella DJ Costs of immune defense: an enigma wrapped in an environmental cloak? Trends Parasitol 2003;*19*(12):571-574.

[61] Triantafilou M, Fradelizi D, Triantafilou K Major histocompatibility class one molecule associates with glucose regulated protein (GRP) 78 on the cell surface. Hum Immunol 2001;*62*(8):764-770.

[62] Rao RV, Peel A, Logvinova A, del Rio G, Hermel E, Yokota T, Goldsmith PC, Ellerby LM, Ellerby HM, Bredesen DE Coupling endoplasmic reticulum stress to the cell death program: role of the ER chaperone GRP78. FEBS Lett 2002;*514*(2-3):122-128.

[63] Fedorka KM, Zuk M, Mousseau TA Immune suppression and the cost of reproduction in the ground cricket, Allonemobius socius. Evolution 2004;*58*(11):2478-2485.

[64] Siva-Jothy MT, Tsubaki Y, Hooper RE Decreased immune response as a proximate cost of copulation and oviposition in a damselfly. Physiol Entomol 1998;*23*(3):274-277.

[65] Horak P, Ots I, Tegelmann L, Moller A Health impact of phytohaemagglutinin-induced immune challenge on great tit (Parus major) nestlings. Canadian Journal of Zoology-Revue Canadienne De Zoologie 2000;*78*(6):905-910.

Tables

Table 1. Multiple ANOVA analysis applied to 2D-DIGE protein spot relative intensities among old and young mice treated with PBS or LPS

Spot N°	Dependent variables	Acc. N°	Biological process	F	P
110	78 kDa glucose-regulated protein (GRP-78)	gi|2506545	Protein folding & Response to ER stress	9.02	0.0021
180	Dihydrolipoyl dehydrogenase + Prolyl aminopeptidase + Fibrinogen beta chain	gi|118572640 gi|124028616 gi|67460959	Carbohydrate metabolism + Proteolysis + hemostasis & Immune response	3.67	0.0437
214	Mitochondrial aldehyde dehydrogenase	gi|1352250	Response to LPS	8.82	0.0023
271	Sorbitol dehydrogenase precursor	gi|152031591	Carbohydrate metabolism	4.62	0.0227
341	3-hydroxyanthranilate 3,4-dioxygenase	gi|61211578	Tryptophan metabolism	4.24	0.0292
360	Carbonic anhydrase 3	gi|30581036	Response to oxidative stress	4.57	0.0234
362	Carbonic anhydrase 3	gi|30581036	Response to oxidative stress	7.05	0.0055
375	Peroxiredoxin-6	gi|6671549	Response to oxidative stress	11.93	0.0007
378	Glutathione-S-transferase	gi|121747	Response to oxidative stress	5.63	0.0121
379	Glutathione-S-transferase	gi|121747	Response to oxidative stress	5.75	0.0112
452	Fibrinogen alpha isoform 2 precursor + Propanoyl-CoA C-acyltransferase + NADP-dependent malic enzyme	gi|33563252 gi|32130432 gi|162139827	Hemostasis & Immune response + bile acid biosynthesis & fatty acid oxidation + Carbohydrate metabolism	5.76	0.0112
459	Haloacid dehalogenase-like hydrolase domain-containing protein 3	gi|81904469	unknown	10.31	0.0043
469	Glutathione-S-transferase	gi|121747	Response to oxidative stress	4.97	0.0181
491	Glutathione synthetase	gi|1708057	Response to oxidative stress	3.78	0.0403
492	S-adenosylmethionine synthase isoform type-1	gi|81902386	Response to oxidative stress & methylation & S-adenosylmethionine metabolism	3.79	0.0402
507	Glycine N-methyltransferase	gi|55976615	Response to oxidative stress & tumor suppression & S-adenosylmethionine metabolism & immune response	4.45	0.0254
510	Glycerol-3-phosphate dehydrogenase [NAD(+)], cytoplasmic	gi|121557	Carbohydrate metabolism	5.40	0.0139

Multiple ANOVA was conducted on proteomics-derived liver protein levels in old and young mice treated with PBS or LPS (n= 4 in each group). 17 differential protein spots were hence determined ($P < 0.05$), which were considered for subsequent PCA analyses. The biological processes in which each of the proteins from the 17 differential protein spots is involved in were computed using annotation explorer module of the MSDA software suite [43] and complemented with literature examination. Spot N° refers to those reported in Fig 1.

Table 2. Phenotypic responses in immune-challenged (LPS) old and young mice

			PC1	PC2	PC3
Liver oxidative proxies and body mass loss					
	Body mass loss		**0.855**	0.394	
	Glutathione-S-transferase activity		-0.114	**0.967**	
	Total GSH		**0.963**	0.023	
	GSSG		**0.961**	0.014	
	Protein carbonyl		**-0.760**	0.314	
		% variance explained	*0.63*	*0.24*	
Liver protein levels					
Resp. Ox. stress	3-hydroxyanthranilate 3,4-dioxygenase	spot 341	**0.862**	-0.153	-0.321
	Glutathione-S-transferase	spots 378 & 379 & 469	**0.832**	-0.349	-0.005
	Peroxiredoxin-6	spot 375	**0.794**	-0.430	0.190
	78 kDa glucose-regulated protein (GRP-78)	spot 110	**-0.775**	0.397	0.067
	Carbonic anhydrase 3	spots 360 & 362	**0.701**	-0.297	0.454
Resp. Ox. Stress & energy metab.	Glutathione synthetase	spot 491	-0.218	**0.921**	0.154
	S-adenosylmethionine synthase isoform type-1	spot 492	-0.296	**0.889**	0.101
	Sorbitol dehydrogenase precursor	spot 271	0.440	**-0.717**	-0.187
	Fibrinogen alpha polypeptide isoform 2 precursor + Propanoyl-CoA C-acyltransferase + NADP-dependent malic enzyme	spot 452	-0.567	**0.694**	0.101
Resp. Ox. Stress & immune chall.	Mitochondrial aldehyde dehydrogenase	spot 214	-0.101	0.023	**0.878**
	Glycine N-methyltransferase	spot 507	0.201	-0.212	**-0.752**
	Dihydrolipoyl dehydrogenase + Prolyl aminopeptidase + Fibrinogen beta chain	spot 180	0.324	0.162	**0.744**
		% variance explained	*0.33*	*0.27*	*0.19*

Principal Components Analyses were conducted on body mass loss values and liver oxidative proxies, and on proteomics-derived liver protein levels in old and young mice treated with PBS or LPS (n= 4 in each group). For protein levels, only differential 2D-DIGE protein spots (initially recognized on the basis of multiple ANOVA analysis; see Table 1) were considered. Nature of the variables forming the main axes (PC1, PC2 and PC3) allow phenotypic responses to an immune challenge (LPS) to be described compared between old and young mice. Spot N° refers to those reported in Fig 1. Protein loadings over 0.6 (in bold) were considered and allowed principal components to be linked to particular biological processes.

Table 3. GLM applied to PC1, PC2 and PC3 determined for liver protein levels

	Mean values	Estimates	D.F.	F	P
PC1. Response to oxidative stress					
Age (old *vs.* young)		0.026 ± 0.533	1.15	2.090	0.174
Treatment (LPS *vs.* PBS)		-1.467 ± 0.533	1.15	6.346	**0.027**
Age x treatment			1.15	5.997	**0.031**
Old PBS	0.286 ± 0.352		1.7	0.458	0.524
Old LPS	0.663 ± 1.059				
Young PBS	0.259 ± 0.913		1.7	8.407	**0.027**
Young LPS	-1.208 ± 0.436				
PC2. Response to oxidative stress and energy metabolism					
Age (old *vs.* young)		0.118 ± 0.646	1.15	0.311	0.588
Treatment (LPS *vs.* PBS)		1.395 ± 0.646	1.15	5.014	**0.045**
Age x treatment			1.15	0.667	0.430
PC3. Response to oxidative stress and immune challenge					
Age (old *vs.* young)		2.341 ± 0.369	1.15	25.831	**< 0.001**
Treatment (LPS *vs.* PBS)		1.399 ± 0.369	1.15	2.164	0.167
Age x treatment			1.15	15.167	**0.002**
Old PBS	0.979 ± 0.547		1.7	1.853	0.222
Old LPS	0.347 ± 0.750				
Young PBS	-1.362 ± 0.357		1.7	34.376	**0.001**
Young LPS	0.037 ± 0.314				

Generalized linear models were conducted to explain the variance in PC1, PC2 and PC3 determined from proteomics-derived liver protein levels (see Figure 3) in old and young mice treated with PBS or LPS (n=4 in each group). Because both treatment effects and interaction Age x treatment were significant for PC1, and both age effects and interaction age x treatment were significant for PC3, we further conducted post-hoc tests to better characterize differences between groups, by comparing Old PBS *vs.* Old LPS and Young PBS *vs*. Young LPS (in grey). Estimates and mean values are given ± SE and significant values are indicated in bold. Residuals for each models followed a normal distribution (checked using Kolmogorov-Smirnov test and QQ plot).

Table 4. GLM applied to PC1 and PC2 determined for liver oxidative proxies and body mass loss

	Mean values	Estimates	D.F.	F	P
PC1					
Age (old *vs.* young)		0.709 ± 0.184	1.15	0.014	0.757
Treatment (LPS *vs.* PBS)		-1.057 ± 0.261	1.15	11.661	**< 0.001**
Age x treatment			1.15	12.468	**0.004**
Old PBS	1.208 ± 0.538		1.7	4.126	0.089
Young PBS	0.499 ± 0.329				
Old LPS	-1.150 ± 0.131		1.7	4.998	**0.059**
Young LPS	-0.557 ± 0.358				
PC2					
Age (old *vs.* young)		-1.697 ± 0.563	1.15	7.292	**0.019**
Treatment (LPS *vs.* PBS)		-1.173 ± 0.563	1.15	1.921	0.191
Age x treatment			1.15	2.433	0.145

Generalized linear models were conducted to explain the variance in PC1 and PC2 determined from liver oxidative measurements and body mass loss (see Figure 2) in old and young mice treated with PBS or LPS (n=4 in each group). Because both treatment effects and interaction age x treatment were significant for PC1, we further conducted post-hoc tests to better characterize differences between groups, by comparing Old PBS *vs.* Young PBS and Old LPS *vs*. Young LPS (in grey). Estimates and mean values are given ± SE and significant values are indicated in bold. Residuals for each models followed a normal distribution (checked using Kolmogorov-Smirnov test and QQ plot).

Figures

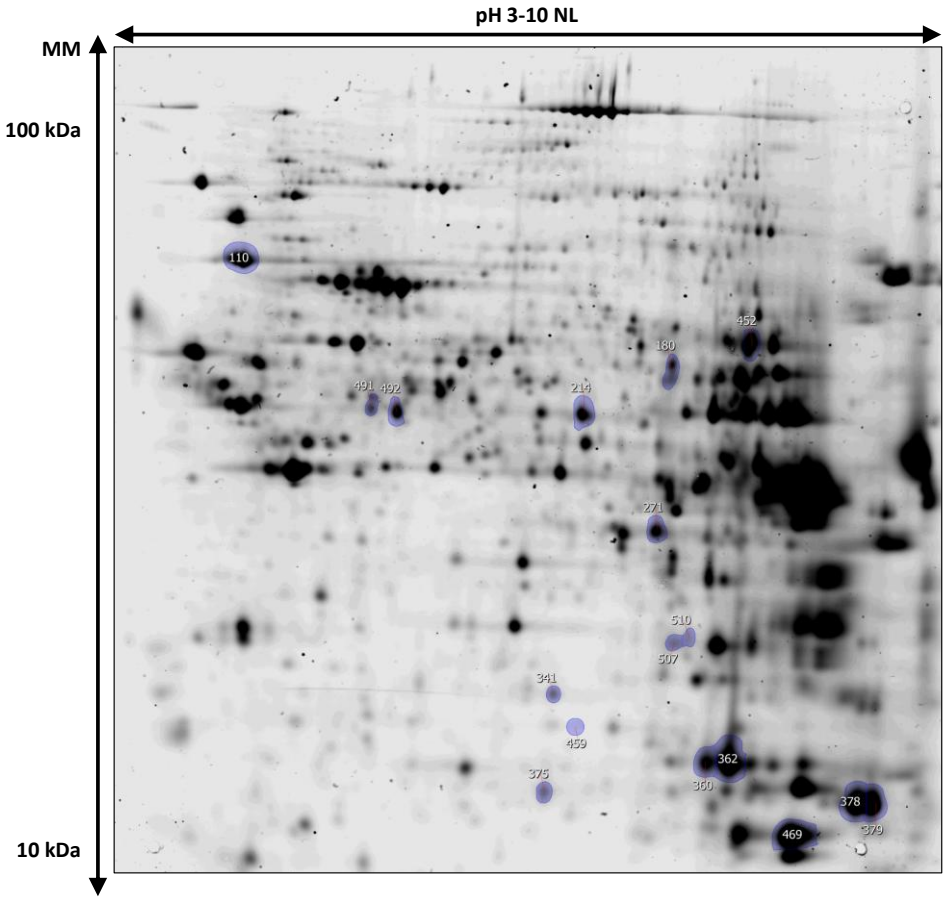

Figure 1 : Representative 2D-gel image of mouse liver proteins
Significantly different protein spots according to multiple ANOVA analysis (P<0.05) are shown.

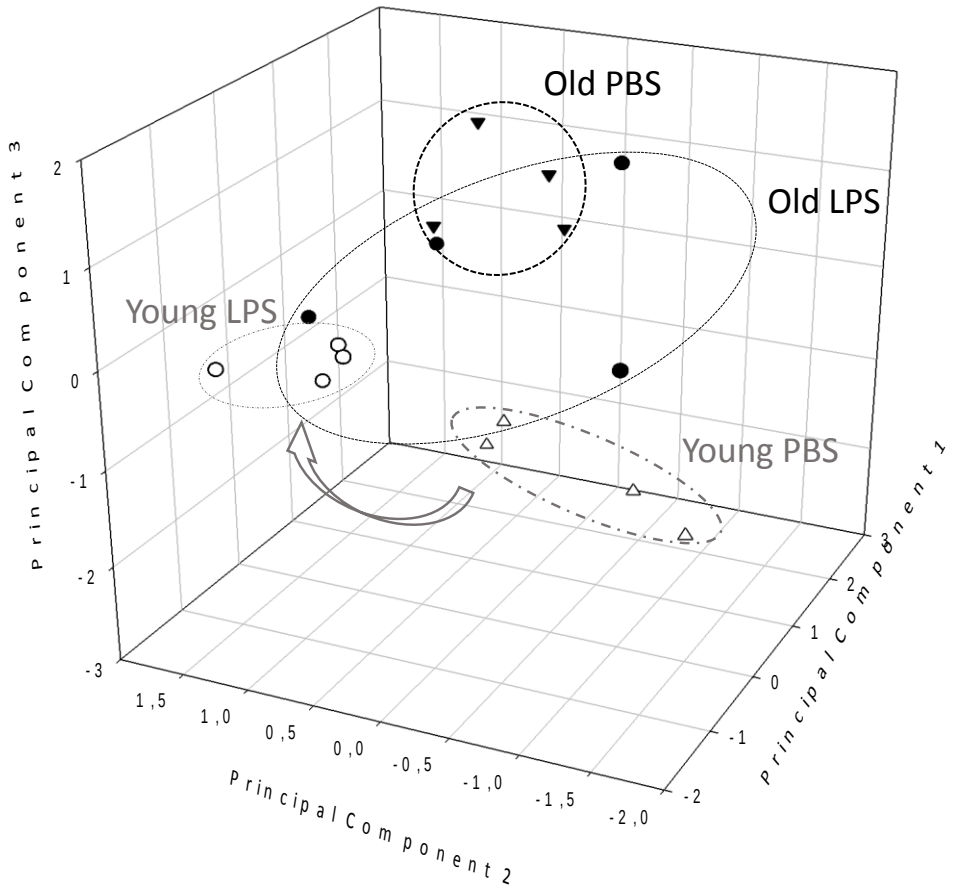

Figure 2 : PCA on proteomics-derived liver protein levels

PCA was conducted on relative protein abundance values for differential 2D-DIGE protein spots (initially recognized on the basis of multiple ANOVA analysis) in old and young mice treated with PBS or LPS (n=4 in each group). Principal components (see Table 2) accounted for a total of 33% (PC1), 60% (PC1+PC2) and 79.7% (PC1+PC2+PC3) of the total variance. Ellipses and arrows indicate how old (black) and young (grey) mice reacted in response to LPS vs. PBS treatment.

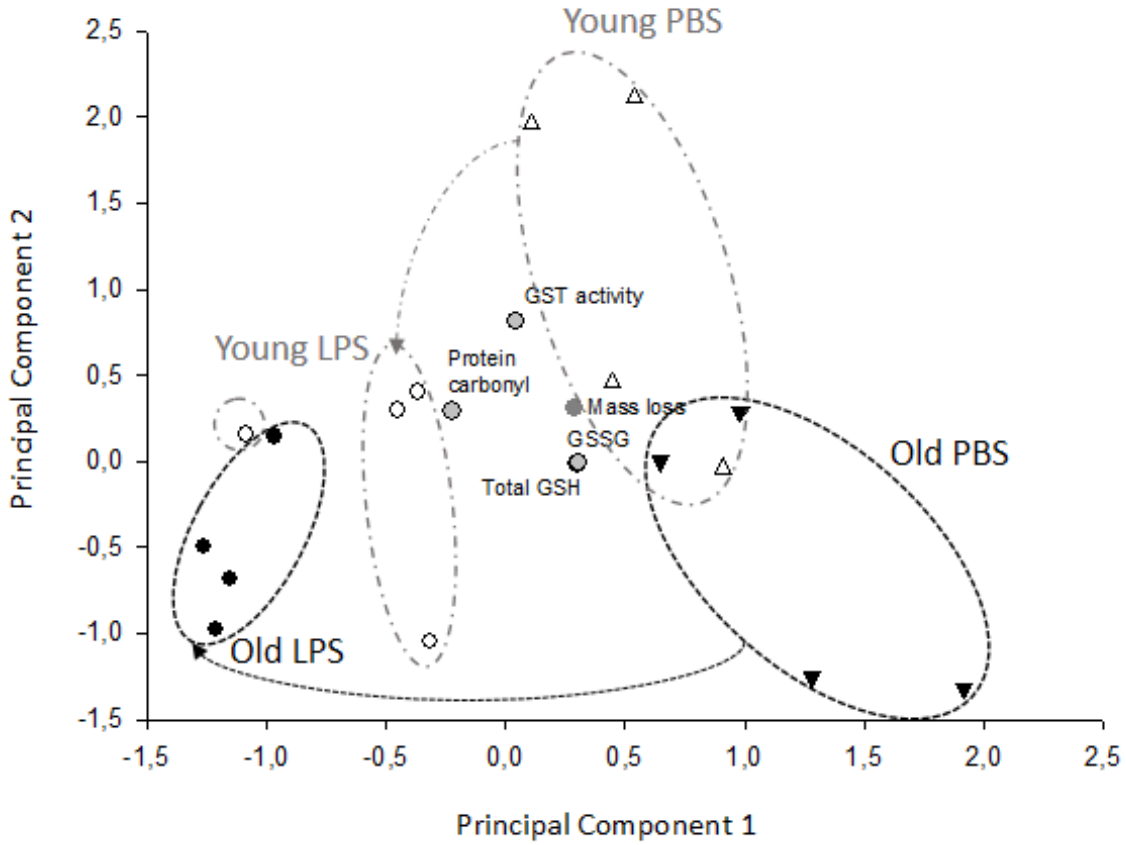

Figure 3 : PCA on liver oxidative proxies and body mass loss

PCA was conducted on liver oxidative measurements and body mass loss recorded in old and young mice treated with PBS or LPS (n=4 in each group). Indicated by grey points, age and oxidative balance proxies (GST activity, protein carbonyl, total GSH and GSSG contents), as well as body mass loss are projected onto their first two principal components (see Table 2) accounting for a total of 63.6% (PC1) and 87.4% (PC1+PC2) of the total variance. Ellipses and arrows indicate how old (black) and young (grey) mice reacted in response to LPS vs. PBS treatment.